MAGNETIC ANOMALIES ON THE TREE TRUNKS

GUNTHER KLETETSCHKA[1,2], VOJTĚCH ŽILA[3] AND PETER J. WASILEWSKI[1]

1 Code 691, NASA Goddard Space Flight Center, Greenbelt, Maryland, USA (gunther@core2.gsfc.nasa.gov)
2 Howard University, 400 Bryant St. Washington DC, USA
3 Charles University, Albertov 6, 128 43 Prague 2, Czech Republic

Received: April 10, 2002; Accepted: February 19, 2003

ABSTRACT

Magnetic measurements of soil and tree bark adjacent to a busy highway revealed a significant variation in the concentration of magnetic particles with distance from the highway. Further more, forest-facing tree-bark contains significantly more magnetic particles than road-facing tree-bark. Magnetic particles were detected both on the bark of the maple trees and in the first centimeter of the soil cover (O/A horizon). Stability of saturation isothermal magnetization (SIRM) and hysteresis parameters of the soil indicates the presence of single domain (SD/PSD) magnetic carriers. Measurements of the tree bark hysteresis parameters and SIRM detect a significant lower coercivity component that we interpret to be an indication of more abundant pseudo-single domain (PSD) type magnetic grains. Magnetic measurements around the perimeters of eight tree trunks reveal magnetic carriers whose distribution is antipodal to the source direction (highway). We interpret our observation by adopting an air circulation model, where suspended PSD/SD particles are carried in the air stream. The air stream from the heavy traffic lowers the amount of moisture on the tree trunk surfaces facing the highway and thus reduces an adhesive potential on this side. Therefore, more particles can stay on the moist side of the trunk protected from the direct airflow.

Keywords: environment, pollution, soil, wood, iron oxides, hysteresis loops

1. INTRODUCTION

The provenance, distribution, and localization of human contamination can be effectively described by utilization of magnetic measurements. We address this issue here by reporting on a curious antipodal effect on tree trunks near busy highways. We invoke an atmospheric circulation model to explain the location of magnetic particles antipodal to the highway facing part of the tree trunk.

Our objective was to confirm that heavy traffic has a measurable magnetic effect on surrounding vegetation surfaces. Contamination by air-borne ash in industrial areas is often reported to be easily detectable by magnetic techniques (*Heller et al., 1998*; *Kapička et al., 2000*; *Kapička et al., 2001*; *Kapička et al., 1999*; *Lecoanet et al., 2001*; *Magiera* *and Strzyszcz, 2000*; *Schmidt et al., 2000*; *Strzyszcz, 1999*). Apart from pollution of coal-burning power plants we are considering pollution of heavy traffic common in highly industrial areas near large cities. The Washington - Baltimore Parkway is an example of a highway carrying millions of cars (no trucks) each year. Cars wear down at a rate proportional to both the age and the worsening car condition. Highways with high-density traffic crossing the wildlife preserves may accumulate more material from car erosion than local city streets with less traffic.

2. MATERIAL AND METHODS

We chose our sample area along the Washington-Baltimore Parkway, a major highway connecting the two large cities where trucks are prohibited from this road. The collecting area was just north of the exit to the Goddard Space Flight Center, MD at N39º00.55’, W76º51.72’ (geographical coordinates). Samples of soil and tree bark (Red Maple, *Acer Rubrum*) were collected along a profile starting from the edge of the road (end of the shoulder pavement) and extending about 20 m into the adjacent area covered with deciduous trees. At first, five soil samples and ten tree-bark samples were collected from the eastern side of the highway. Two bark samples were collected from each tree. One sample was from the forest-facing side of the tree and the other from the road-facing side. After detecting the antipodal magnetic signature pattern on the tree-bark samples, we collected an additional two soil and four tree-bark samples from the western side of the highway to confirm that the presence of the highway causes the observed pattern. Samples of soil contained the uppermost horizon (not exceeding depth of 1 cm) containing mostly organics (O-horizon). Tree bark was scraped with a commercial steel scraper and collected above 30 cm and below 160 cm from the ground. Scraping did not remove more than a 1mm thick layer of the tree-bark tissue. Contamination from our scraper could not contribute to saturation magnetization measurements with more than 10^{-3} Am^2kg^{-1} (magnetization of the road facing tree bark, see discussion). Samples of soil and tree bark were placed into plastic containers (~15 cm^3), sealed (to prevent loss of the moisture content) and tested for magnetic hysteresis properties. Hysteresis loops were obtained with Vibrating Sample Magnetometer (VSM) with a LAKE SHORE controller. Maximum available field was ±2 T. The stability of the saturation remanence was tested with alternating field demagnetization up to 0.24 T and measured using a super-conducting rock magnetometer. Magnetic measurements were completed within a week after the samples were collected.

One larger tree (trunk approximately 30 cm in diameter) was used for measurements of magnetic susceptibility variation along its circumference at a height of 40 cm above the forest floor. These susceptibility measurements were done with portable instrument, magnetic susceptibility meter SM20 (Geofyzika a.s.) with a sensitivity of 10^{-6} SI.

Table 1. Hysteresis parameters for soils (mXs) and tree bark facing forest (MXbf) samples. “Side” indicates side of the highway from which the samples were collected. Distance is measured between the base of the tree and start of the pavement perpendicular to the highway. H_c is magnetic coercivity. J_s is saturation magnetization. *SIRM* is saturation remanence.

Sample	Side	Distance [m]	H_c [mT]	J_s [Am^2kg^{-1}]	*SIRM* [Am^2kg^{-1}]
m1s	Eastern	6.2	12.6	27.6×10^{-3}	36.4×10^{-4}
m2s	Eastern	8.3	12.3	21.3×10^{-3}	24.6×10^{-4}
m3s	Eastern	11.2	10.6	16.2×10^{-3}	30.2×10^{-4}
m4s	Eastern	13.3	12.8	15.9×10^{-3}	34.6×10^{-4}
m5s	Eastern	19.3	10.5	16.5×10^{-3}	57.9×10^{-4}
m6s	Western	8.1	11.9	12.6×10^{-3}	25.6×10^{-4}
m7s	Western	9.7	10.6	5.4×10^{-3}	19.6×10^{-4}
m1bf	Eastern	6.2	4.2	0.45×10^{-3}	1.03×10^{-4}
m2bf	Eastern	8.3	9.3	0.75×10^{-3}	1.13×10^{-4}
m3bf	Eastern	11.2	6.5	1.53×10^{-3}	2.03×10^{-4}
m4bf	Eastern	13.3	7.0	1.38×10^{-3}	1.45×10^{-4}
m5bf	Eastern	19.3	2.0	0.27×10^{-3}	3.22×10^{-4}
m6bf	Western	8.1	5.4	1.53×10^{-3}	2.48×10^{-4}
m7bf	Western	9.7	8.5	0.87×10^{-3}	1.49×10^{-4}

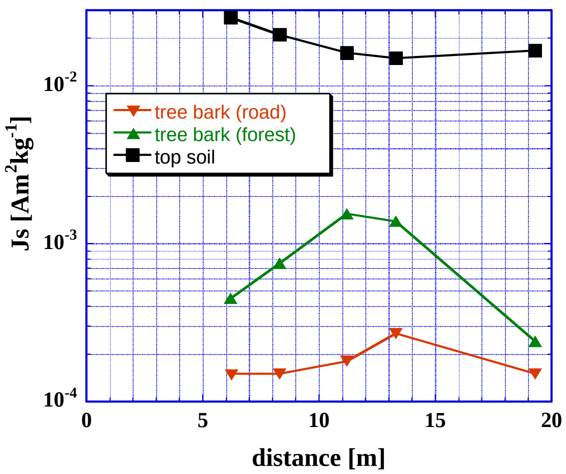

Fig. 1. Magnetic profiles of tree bark (red maple) and soil samples. Note significantly enhanced magnetization of the tree bark facing towards the forest (away from the road).

3. RESULTS

3.1. Soil samples

Hysteresis parameters for the soil samples are listed in Table 1. Fig. 1 illustrates the J_s variability of the soil samples as we increase the distance from the edge of the road. J_s has the largest value 27.6×10^{-3} Am^{2}kg^{-1} for the sample closest to the road (6 m). With the distance increase J_s dropped down to about 15.9×10^{-3} Am^{2}kg^{-1} and 16.5×10^{-3} Am^{2}kg^{-1} at distances 13.3 m and 19.3 m respectively. Coercivity stayed between 10 and 13 mT (Table 1). *SIRM* values ranged between 25×10^{-4} and 60×10^{-4} Am^{2}kg^{-1} and were subsequently demagnetized by alternating magnetic field (Fig. 2). There was no clear dependence of *SIRM* as a function of distance from the road. Saturation magnetization was stable and it took about 30 mT alternating magnetic field to reduce the *SIRM* to half of its original value.

3.2. Tree bark samples

J_s of the forest-facing tree-bark samples increased to its maximum value 1.53×10^{-3} Am^{2}kg^{-1} at the distance of about 11 m from the road and then dropped to its lowest value 0.27×10^{-3} Am^{2}kg^{-1} at 19 m distance. J_s of the road-facing tree-bark samples was close to the VSM instrument resolution and thus embodies at least 20% of the measurement error. J_s also increased to its maximum at 13 m distance and stayed at values less than 2×10^{-4} Am^{2}kg^{-1} for the rest of the samples. Demagnetization of

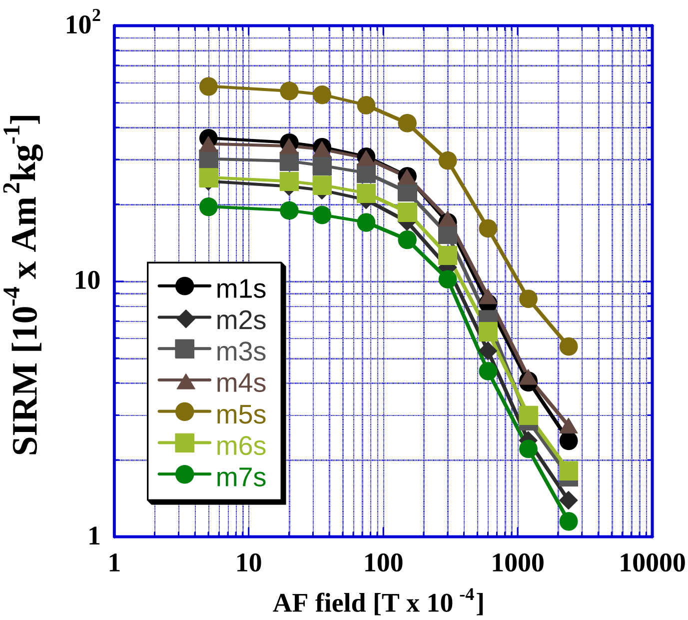

Fig. 2. Alternating magnetic field *SIRM* demagnetization of the soil samples.

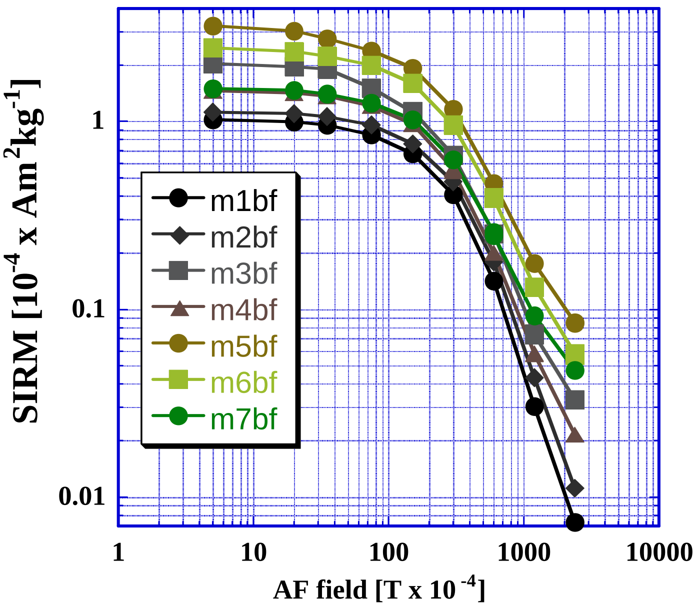

Fig. 3. Alternating magnetic field *SIRM* demagnetization of the forest-facing tree-bark samples.

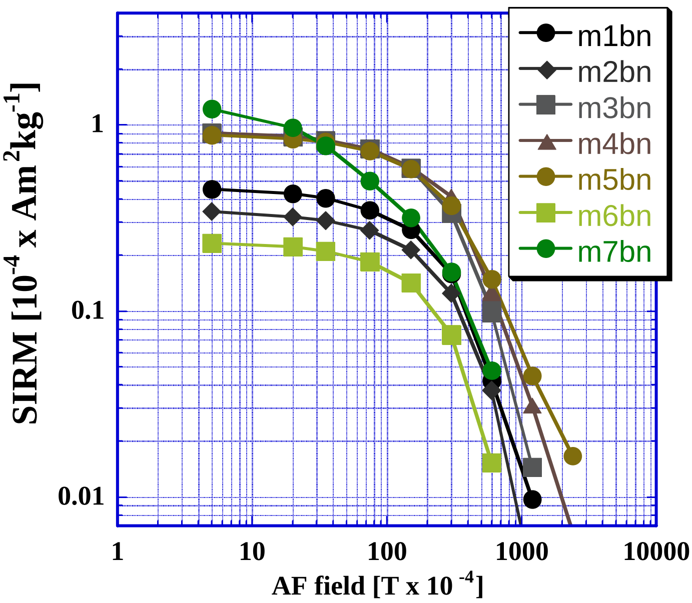

Fig. 4. Alternating magnetic field *SIRM* demagnetization of the highway-facing tree-bark samples

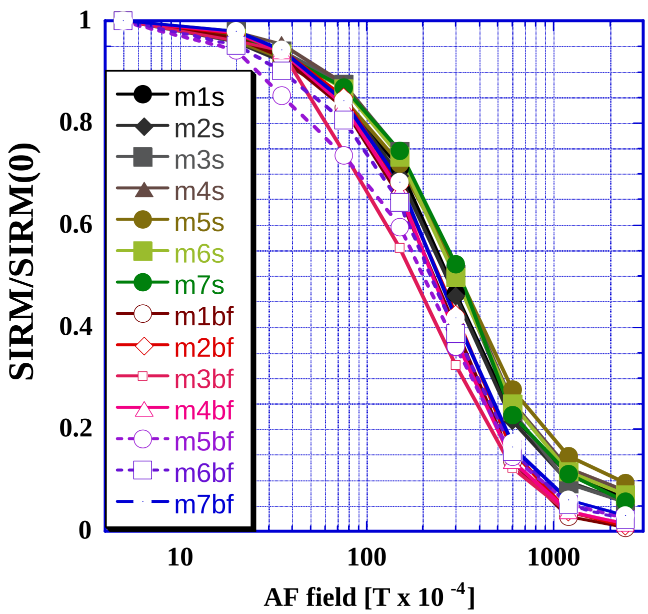

Fig. 5. Normalized demagnetization of *SIRM* of seven soil samples (solid symbols) and seven forest-facing tree-bark samples (empty symbols).

tree-bark samples' *SIRM* is shown in Fig. 3 (forest-facing tree-bark samples) and Fig. 4 (road-facing tree-bark samples). Fig. 5 shows normalized demagnetization curves for soil and tree-bark samples. Tree-bark samples require only ~20 mT to reduce *SIRM* to the half as oppose to ~30 mT required for the soil samples.

Magnetic susceptibility measurements around a trunk of the larger red maple tree (~30 cm in diameter) revealed an asymmetric pattern (Fig. 6). Magnetic susceptibility on the tree side facing the road was about -3.5×10^{-6} as oppose to -2.7×10^{-6} on the tree-side facing the forest. This tree was located on the western side of the highway at the distance of about 6 m from the road shoulder pavement.

4. DISCUSSION

As we expected the soil samples closest to the road (6 m) contained the largest amount of contamination due to proximity to the traffic. Hysteresis loops of natural materials are sensitive mostly to magnetite content, which is the most common form of oxidized iron on Earth. Even a large content (100 times more than magnetite) of another common mineral, hematite, is essentially invisible in magnetic hysteresis analysis and/or susceptibility measurements (*Kletetschka, 1994*; *Kletetschka et al., 2000*) due to the large difference between the J_s of magnetite (90 Am^2kg^{-1}) and hematite (0.4 Am^2kg^{-1}). Because J_s of pure magnetite is well established (~90 Am^2kg^{-1}), the J_s of samples can be used to estimate approximate possible magnetite concentration. In principle some of the particles carried by air could be more reduced because cars are made of steel. However, our

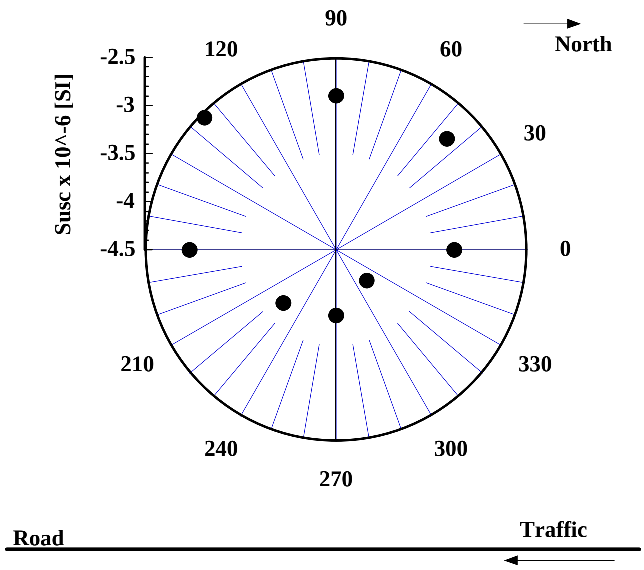

Fig. 6. Magnetic susceptibility measurements around the circumference of a tree trunk 30 cm in diameter. Note that the north direction is to the right. Lower line indicates the highway position in respect to susceptibility measurements. The arrow in the lower right corner indicates the approaching traffic direction.

hysteresis measurements indicate sub-micron size magnetite grains and therefore the large active surfaces of iron would cause quick oxidization to magnetite and/or hematite.

Because we collected samples from both eastern and western sides of the road we have fairly good control as to whether any magnetic increase is due to local factors within a soil or if it is related to the traffic. Our data in Table 1 and Fig. 1 clearly show that Js and thus the assumed possible magnetite concentration increases with the proximity of the road. The magnetic content increase with distance, from about 6.2 to 11.2 m, is reflected as 11.4×10^{-3} Am^{2}kg^{-1} of J_S increase (Table 1) and thus by an additional 0.1 g of possible magnetite per kg of the uppermost material of the soil (depth < 1 cm).

Distributed abundance of this iron rich material in the uppermost organic layer may promote reactions that may have various effects on the plants and bacteria that use this soil for cellular growth. Consequently the next step would be to identify the magnetic species. The presence of metallic contamination may interfere with the growth pattern in the vicinity of the highway. The presence of the fine metallic grains both in the soil and on the plants may have significant effects on expression of metal transporter genes and may cause unwanted changes (*Assuncao et al., 2001*; *Badar et al., 2000*; *Ghaderian et al., 2000*; *Han et al., 2000*; *Silver and Phung, 1996*).

We consider that the steel scraper material may have contaminated the tree-bark samples. The maximum possible extent would be in case where the road-facing bark has no magnetic carriers and all we see is the steel scraper contamination. In this extreme case the forest-facing samples would also carry about the same amount of steel scraper contamination. Then all of the additional contamination of the forest-facing samples must be due to traffic from the highway.

In order to explain the tree-bark magnetization asymmetry increase with distance we propose an air circulation model driven by the high-speed traffic on the highway to explain the observed magnetic pattern. The ferromagnetic fine particles are entrained in the "high velocity" wind. Encountering the trees enables turbulence behind the trees, lowering the velocity and consequently allowing the magnetic particles to be deposited on the tree bark. Magnetism is lower near the road because air circulation is intense not allowing magnetic particles to settle. With increasing distance from the road (10 m) the air speed is low enough to allow magnetic particles to settle on the tree bark. The tree bark surface facing the highway is exposed to the drying effect of the "high velocity" air stream. The backside of the tree would be moist, consequently providing a sticking surface for magnetic particles.

SIRM resistance against alternating field demagnetization (Fig. 5) indicates that the magnetic carriers are very stable and require AF fields as high as 20 mT to demagnetize to 50% of *SIRM*. This value is slightly lower than field that is required to demagnetize the soil particles. This stability indicates mostly SD/PSD magnetic carriers in both materials with grain size close to 0.5 µm. Particles of this size are easily suspended in airflow and concur with our model hypothesis. However, both hysteresis parameters (Fig. 1, Table 1) and *SIRM* demagnetization (Fig. 5) indicate lower coercivity for the bark material. This suggests coarser magnetic grain size on the tree barks. These grain sizes would span into the pseudo-single-domain magnetic region based on $SIRM/J_S$ ratios (Table 1) (*Day et al., 1977*). This observation indicates that magnetic grains trapped on the bark undergo less degree of weathering than the particles on the soil surface. Weathering and oxidation decreases the effective magnetic size of the carriers. Soil surface, in general, is moister and thus promotes more intense weathering than on the dryer tree-bark surfaces.

Negative values of the magnetic susceptibility survey of the larger tree trunk detect the diamagnetic signature of the carbon in the wood. However, diamagnetism varies around the tree (Fig. 6) with the lowest values on a side facing away from the road suggesting a presence of small amount of ferromagnetic particles. The observed asymmetry is consistent with our magnetic observation on smaller trees and indicates an increase of the content of ferromagnetic particles. This observation supports our atmospheric model.

5. CONCLUSIONS

Magnetic screening of the soil and arboreal vegetation (notable maple trees) in vicinity of a highway with heavy traffic reveals a measurable magnetic contamination likely associated with the vehicle traffic. Contamination of the soil is the heaviest just next to the road and rapidly decreases with distance into the tree area. The concentration change across the measured profile is estimated as 0.1 g per kilogram of the uppermost soil material. Tree bark measurements reveal an interesting antipodal magnetic expression with magnetic enhancement on the opposite side in relation to the magnetic influx. An air-circulation model driven by traffic and humidity variations can explain this pattern. This mechanism must be taken into consideration when studying the spread of disease by aerosol in agricultural and forest industry.

References

Assuncao A.G.L., Martins P.D., De Folter S., Vooijs R., Schat H. and Aarts M.G.M., 2001. Elevated expression of metal transporter genes in three accessions of the metal hyperaccumulator Thlaspi caerulescens. *Plant Cell and Environment*, **24**, 217–226.

Badar U., Ahmed N., Beswick A.J., Pattanapipitpaisal P. and Macaskie L.E., 2000. Reduction of chromate by microorganisms isolated from metal contaminated sites of Karachi, Pakistan. *Biotechnology Letters*, **22**, 829–836.

Day R., Fuller M. and Schmidt V.A., 1977. Hysteresis properties of titanomagnetites: grain–size and compositional dependence. *Phys. Earth Planet. Inter.*, **13**, 260–266.

Ghaderian Y.S.M., Lyon A.J.E. and Baker A.J.M., 2000. Seedling mortality of metal hyperaccumulator plants resulting from damping off by Pythium spp. *New Phytologist*, **146**, 219–224.

Han F.X., Kingery W.L., Selim H.M. and Gerard P.D., 2000. Accumulation of heavy metals in a long–term poultry waste– amended soil. *Soil Science*, **165**, 260–268.

Heller F., Strzyszcz Z. and Magiera T., 1998. Magnetic record of industrial pollution in forest soils of Upper Silesia, Poland. *J. Geophys. Res.–Solid Earth*, **103**, 17767–17774.

Kapička A., Jordanova N., Petrovský E. and Ustjak S., 2000. Magnetic stability of power–plant fly ash in different soil solutions. *Phys. Chem. Earth A–Solid Earth and Geodesy*, **25**, 431–436.

Kapička A., Petrovský E., Jordanova N. and Podrázský V., 2001. Magnetic parameters of forest top soils in Krkonose Mountains, Czech Republic. *Phys. Chem. Earth A–Solid Earth and Geodesy*, **26**, 917–922.

Kapička A., Petrovský E., Ustjak S. and Macháčková K., 1999. Proxy mapping of fly–ash pollution of soils around a coal– burning power plant: a case study in the Czech Republic. *J. Geochem. Explor.*, **66**, 291–297.

Kletetschka G., 1994. *A Study of the Origin and Nature of Secondary Iron Oxides in Chinese Loess*. Master thesis. University of Minnesota, Minneapolis.

Kletetschka G., Wasilewski P.J. and Taylor P.T., 2000. Hematite vs. magnetite as the signature for planetary magnetic anomalies? *Phys. Earth Planet. Inter.*, **119**, 259–267.

Lecoanet H., Léveque F. and Arnbrosi J.P., 2001. Magnetic properties of salt–marsh soils contaminated by iron industry emissions (southeast France). *J. Appl. Geophys.*, **48**, 67–81.

Magiera T. and Strzyszcz Z., 2000. Ferrimagnetic minerals of anthropogenic origin in soils of some Polish national parks. *Water Air Soil Pollut.*, **124**, 37–48.

Schmidt M.W.I., Knicker H., Hatcher P.G. and Kogel–Knabner I., 2000. Airborne contamination of forest soils by carbonaceous particles from industrial coal processing. *J. Environ. Quality*, **29**, 768–777.

Silver S. and Phung L.T., 1996. Bacterial heavy metal resistance: New surprises. *Annual Review of Microbiology*, **50**, 753–789.

Strzyszcz Z., 1999. Heavy metal contamination in mountain soils of Poland as a result of anthropogenic pressure. *Izvestiya Akademii Nauk Seriya Biologicheskaya*, **6**, 722–735.